

Synthesis of antihyperglycemic, α -glucosidase inhibitory, and DPPH free radical scavenging furanochalcones

R. Ranga Rao · Ashok K. Tiwari · P. Prabhakar Reddy · K. Suresh Babu ·
G. Suresh · A. Zehra Ali · K. Madhusudana · Sachin B. Agawane ·
Preethi Badrinarayan · G. Narahari Sastry · J. Madhusudana Rao

Received: 16 September 2010 / Accepted: 19 January 2011 / Published online: 8 February 2011
© Springer Science+Business Media, LLC 2011

Abstract A series of furanochalcone derivatives have been designed and synthesized. Molecular modeling studies were carried out to probe into the mechanism of binding of chalcone inhibitors and understand the structure–activity relationship to identify the contribution of scaffolds and groups in the synthesized analogs to biological activity. The three-dimensional model of α -glucosidase was constructed based on the crystal structure family 31 α -glycosidase (PDB 1XSI) using Modeller9v5. Docking of the inhibitors on the built homology model revealed interactions in the active site region mostly with Asp 252, Tyr254, Gln523, and Arg571. 2D-QSAR models were generated with CODESSA using Heuristic method. The best predictive model was generated using three descriptors that gave a correlation co-efficient (r^2) 0.9886 and cross-validate (r^2) 0.9338. The synthesized compounds were screened against the α -glucosidase inhibition and DPPH radical scavenging properties. All the synthetic compounds displayed varying degrees of α -glucosidase inhibitory and DPPH scavenging activities. Compound **8c** was found most potent α -glucosidase inhibitor though; it could not display DPPH

scavenging activity. When tested in vivo for antihyperglycemic activity in starch-loaded Wistar rats, **8c** was equally effective in reducing time-dependent hyperglycemia as to the standard drug, Acarbose. Compound **8c** may serve as an interesting compound for the development of therapeutics targeted against diet-induced hyperglycemia in diabetes.

Keywords Furanochalcones · DPPH free radical scavenging activity · α -Glucosidase inhibitory activity · Molecular modeling · QSAR

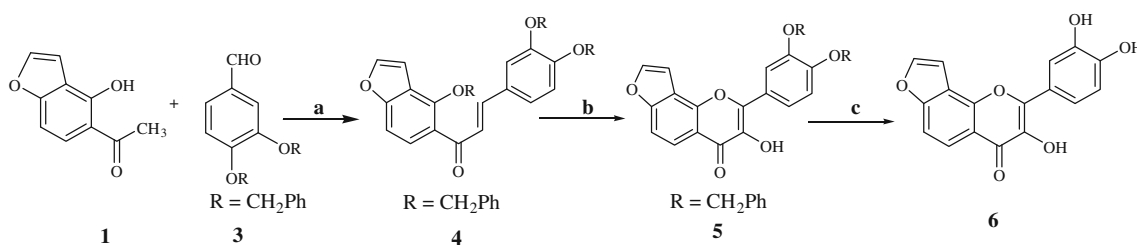
Introduction

Food carbohydrates constitute major source of energy in the diet of South Asians, Asian Indians in particular (Mohan *et al.*, 2009; Mishra *et al.*, 2009). Consumption of carbohydrate-rich foods lead to the rapid rise in postprandial blood glucose level. Review on daily seven-point blood glucose profile monitoring in patients subpopulation from five different geographic regions of the world, showed that Indians demonstrate significantly high level of postprandial hyperglycemia (PPHG) when compared with other subpopulations (Milisevic *et al.*, 2008). PPHG now has been established as one of the earliest detectable abnormalities expressed in ensuing diabetes mellitus (Gerich, 1996), better predictor of progression of diabetes (Davidson, 2003), cardiovascular diseases (CVD) and an independent risk factor for atherosclerosis (Boutati and Raptis, 2004). It has also been implicated in inducing oxidative stress (Ceriello, 2008) that is recognized as a major pathophysiological link between cardiovascular disorders and diabetes (Giugliano *et al.*, 1996). Therefore, mitigation of rapid postprandial hyperglycemic excursion

R. Ranga Rao · P. Prabhakar Reddy · K. Suresh Babu ·
G. Suresh · J. Madhusudana Rao (✉)
Natural Products Laboratory, Division of Organic Chemistry-I,
Indian Institute of Chemical Technology, Uppal Road,
Hyderabad 500 607, India
e-mail: janaswamy@iict.res.in

A. K. Tiwari · A. Z. Ali · K. Madhusudana · S. B. Agawane
Division of Pharmacology, Indian Institute of Chemical
Technology, Uppal Road, Hyderabad 500 607, India

P. Badrinarayan · G. Narahari Sastry
Molecular Modelling Group, Organic-I Division, Indian Institute
of Chemical Technology, Uppal Road,
Hyderabad 500 607, India



Scheme 1 Reagents and condition: **a** KOH (60%), EtOH, 75%, 24 h; **b** H₂O₂, NaOH, 0°C, 12 h, 45%; (**c**) TiCl₄, -10°C, 15 min, dry DCM, 64%

(PPHGE) holds promise in reducing the risk for development of diabetes, CVD, and oxidative stress and has been proved by the evidence of reducing PPHGE by intervention with intestinal α -glucosidase inhibitor drug Acarbose (Delorme and Chiasson, 2005; Yamagishi *et al.*, 2005).

Natural agents that retard and/or delay the absorption of carbohydrates are now becoming practical strategies (McCarty, 2000) and logical way (Matsui *et al.*, 2006; Aparna *et al.*, 2009) for the search of new pharmacological agents for prevention of PPHGE. In the course of our efforts in identifying antihyperglycemics from traditional Indian medicinal plants, we reported recently new intestinal α -glucosidase inhibitor furanoflavonoids from antihyperglycemic extract of *Derris indica* Lam (Leguminosae) (Rao *et al.*, 2009). In the process of reconfirmation of the structure of a new furanoflavonoid 3,3',4'-trihydroxy-4H-furo[2,3-*h*]chromen-4-one (**6**) through synthetic approach, we observed that furanochalcone (**4**), the intermediate in synthetic route (Scheme 1) displayed better intestinal α -glucosidase inhibitory activity than the new compound. This observation led us to synthesize several new furanochalcones. We report herein synthesis of new furanochalcones and their ability of inhibiting rat intestinal α -glucosidase and 1,1-diphenyl-2-picrylhydrazyl (DPPH) free radical scavenging activities. Our earlier studies employing homology modeling, (Murthy *et al.*, 2005; Chourasia *et al.*, 2005; Reddy *et al.*, 2006) docking (Ravindra *et al.*, 2008), QSAR (Srivani and Sastry, 2009) were helpful in examining the interactions of the synthesized inhibitors with α -glucosidase and develop structure–activity relationship. We also report antihyperglycemic activity of most potent α -glucosidase inhibitor in starch-induced PPHG in rats. This is the first report identifying furanochalcones possessing α -glucosidase inhibitory, DPPH scavenging and antihyperglycemic activities.

Chemistry

Results and discussion

Furanoflavonoid (**6**) was synthesized in three steps (Scheme 1). The Claisen–Schmidt condensation of substituted

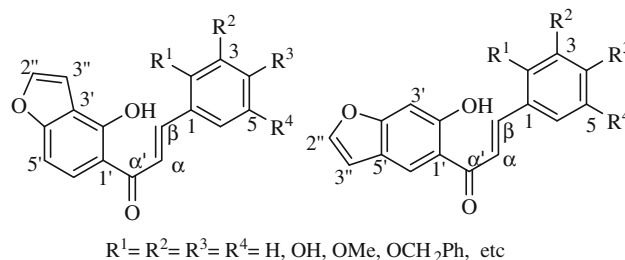


Fig. 1 General chemical structures of targeted chalcones

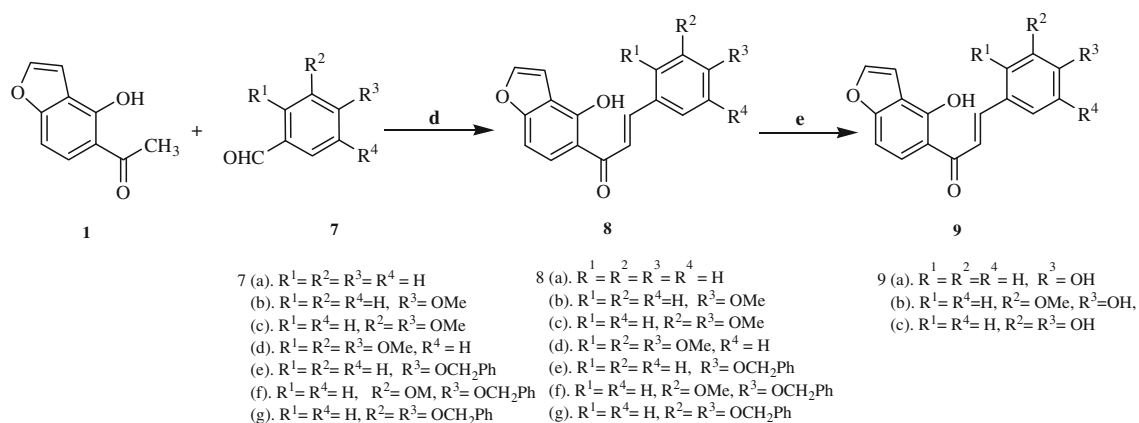
benzaldehyde (**3**) and acetophenone derivative (**1**) (Goel and Dixit, 2004) in presence of aqueous potassium hydroxide produced corresponding chalcone (**4**) (Rao *et al.*, 2009). Resulted chalcone was converted to benzylated furanoflavonoid (**5**) using Algar–Flynn–Oyamada reaction (Zhitao *et al.*, 2008) by treatment with alkaline hydrogen peroxide. Further, it was debenzylated using TiCl₄ (Selvam *et al.*, 2009) in dry DCM under N₂ atmosphere affording 3,3',4'-trihydroxy-4H-furo[2,3-*h*]chromen-4-one (**6**) (Scheme 1; Fig. 1).

Claisen–Schmidt condensation of acetophenone derivative (**1**) (Goel and Dixit, 2004) with various substituted benzaldehydes (**7a–7g**) in the presence of aqueous KOH in anhydrous ethanol-reduced angular furanochalcones [(**8a–8g**), Scheme 2]. Amongst angular furanochalcones, some benzyl protected chalcones (**8e–8g**) were further debenzylated using TiCl₄ in dry DCM for 15 min under N₂ atmosphere to afford angular hydroxy furanochalcones (**9a–9c**), respectively.

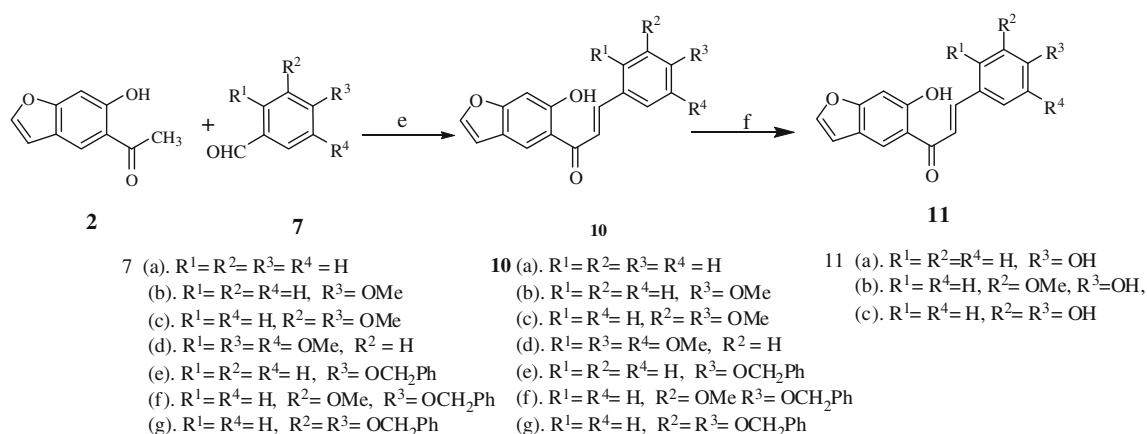
Claisen–Schmidt condensation of acetophenone derivative (**2**) (Goel and Dixit, 2004) with different substituted benzaldehydes (**7a–7g**) in the presence of aqueous potassium hydroxide in anhydrous ethanol resulted linear furanochalcones (**10a–10g**) (Scheme 3). Amongst linear furanochalcones some benzyl-protected chalcones (**10e–10g**) were further debenzylated using TiCl₄ to afford linear hydroxy furanochalcones (**11a–11c**).

Biological activity

Furanochalcone (**9c**) with hydroxyl groups at third and fourth positions displayed both the potent α -glucosidase



Scheme 2 Reagents and condition: *d* KOH (60%), ethanol, 24 h; *e* TiCl₄, dry DCM, -10°C, 15 min, N₂



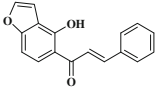
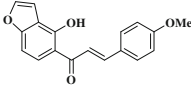
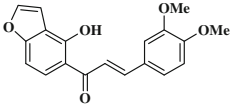
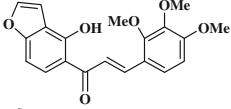
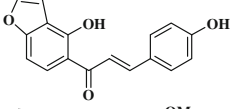
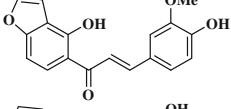
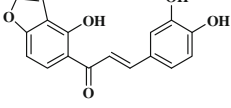
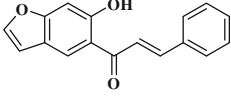
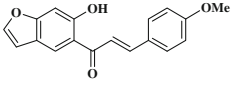
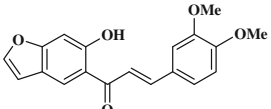
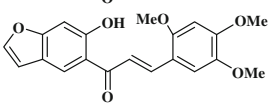
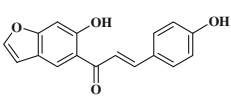
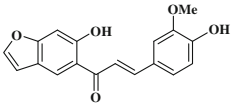
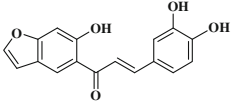
Scheme 3 Reagents and condition: *e* KOH (60%), Ethanol, 75%, 24 h; *f* TiCl₄, dry DCM, -10°C, 15 min, N₂

inhibitory as well as DPPH free radical scavenging activity. With the intact hydroxyl groups at third and fourth positions change in furan ring from angular to linear could not influence change in the activity profile (**11c**). It appears therefore that presence of both hydroxyl groups in compounds **9c** and **11c**; angularity or linearity of the furanoid ring could not influence biological activity of the compounds in agreement with our in silico observations. Absence of hydroxyl group at third position (**9a**) led the improvement of both α -glucosidase inhibitory as well as DPPH free radical scavenging activity. However, absence of both hydroxyl groups (third and fourth positions) drastically reduced the activity as observed in compound **8a**. Contrary to the angular chalcones, absence of hydroxyl group at third position drastically reduced the α -glucosidase inhibitory activity with the improvement of DPPH free radical scavenging potential (**11a**). On the other hand, absence of hydroxyl groups at third and fourth positions (**10a**), we observed loss of free radical scavenging activity with intact of α -glucosidase inhibitory property. On the one

hand, substitution of methoxyl group in compound **8a** at fourth position improved α -glucosidase inhibitory activity (**8b**). Further, substitution of methoxyl group at third position in compound **8c** enhanced IC₅₀ value from 5 μ M to 9.2 μ M for compound **8b**. However, this could not happen in the case of **11c**. Further substitution of methoxy group in angular furanochalcone (**8c**) at second position (**8d**) led to the reduction in α -glucosidase inhibitory activity (IC₅₀, 5.0 μ M vs. 17.32 μ M). We could not observe major difference in α -glucosidase inhibitory activity in linear furanochalcones, while substituting methoxy group and changing the positions of methoxy **10c** when compared with **10d**. Hydroxyl group at fourth position and methoxy group at third position in linear (**11b**) or angular furanochalcone (**9b**) do not change the α -glucosidase inhibitory and DPPH free radical scavenging activity of the compounds. Table 1 shows the IC₅₀ and SC₅₀ values of test compounds.

Recently, American association of clinical endocrinologists/American college of endocrinology consensus panel

Table 1 α -Glucosidase inhibitory and DPPH scavenging activity of furanochalcones

S. no	Structures of liner/ angular chalcones	Yield (%)	% \pm SD for the α -glucosidase inhibition at 25 μ g/ml concentration (IC_{50} ; μ M)	% \pm SD for the DPPH scavenging 20 μ g/ml concentration (SC_{50} ; μ M)
8(a)		70	20.81 \pm 0.	7.57 \pm 2.47
8(b)		85	94.81 \pm 4.14 (9.2)	NA
8(c)		90	89.49 \pm 3.12 (5.0)	NA
8(d)		79	67.26 \pm 4.72 (17.32)	7.3 \pm 0.54
9(a)		68	65.68 \pm 0.32 (10.9)	75.78 \pm 0.67 (17.81)
9(b)		60	45.02 \pm 2.57	54.22 \pm 0.15
9(c)		68	61.48 \pm 0 (15.2)	67.87 \pm 0.82 (29.68)
10(a)		80	67.57 \pm 0.96 (14.5)	9.91 \pm 1.89
10(b)		92	48.90 \pm 2.99	NA
10(c)		91	89.35 \pm 5.1(10.8)	8.78 \pm 0.29
10(d)		86	67.95 \pm 1.17 (13.4)	17.11 \pm 2.75
11(a)		70	8.77 \pm 0.44	73.22 \pm 0.05 (11.96)
11(b)		65	52.82 \pm 1.01	42.08 \pm 1.21
11(c)		54	62.67 \pm 1.41 (18.9)	69.75 \pm 0.19 (26.16)
	Acarbose		55 \pm 1.05 (18.6)	
	Trolox		–	99.5 \pm 0.12 (4.8)

on type 2 diabetes mellitus has advocated that α -glucosidase inhibitors are most effective in reducing PPHG in typical Asian dietary conditions (Zhitao *et al.*, 2008). Its use is also associated with a slight decrease in fasting glucose concentrations. The α -glucosidase inhibitors have been observed to improve overall glycemic control and reduction of glucose toxicity. It has further been reported that reduction of PPHG also reduces the postprandial burden of oxidative stress (Delorme *et al.*, 2005; Yamagishi *et al.*, 2005). Based on these determinants, we selected the most potent α -glucosidase inhibitor (**8c**) for the study of antihyperglycemic activity in starch-induced post-prandial hyperglycemic rats. It is evident from (Fig. 2a) that compound **8c** was equally effective in reducing time-dependent hyperglycemic burden as to the standard drug, Acarbose. Similarly, compound **8c** equally mitigated overall hyperglycemic burden in terms of area under the curve (AUC) in starch-induced hyperglycemia in rats as that in the case of acarbose (Fig. 2b).

Molecular modeling studies

Homology modeling

The determination of secondary structure with STRIDE reveals the presence of 9 helices, 47 β -sheets and many intermittent coils (Fig. 3). The built model has approximately 90% in favoured, 7% in allowed, and 2% in outlier region of Ramchandran plot (Fig. 4a). ProSA gave a Z score of -3.03 (Fig. 4b). Verification of the model with *what if* shows fulfillment of spatial constraints to a satisfactory level. Visualization of the model confirmed the modeling of the active site with minimum variation thus validating its use as receptor for docking.

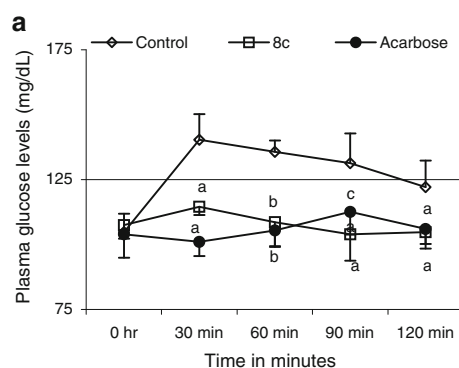
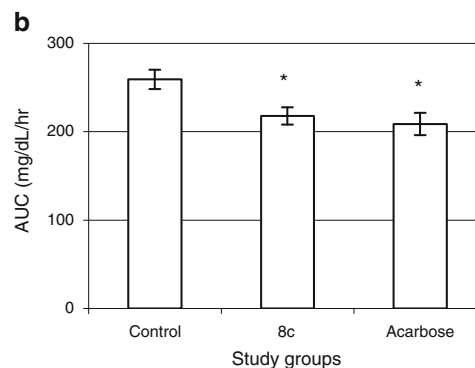


Fig. 2 Antihyperglycemic activity of test compound **8c** in rats. **a** Plasma glucose levels of rats after starch feeding at different time points in animals of various groups. **b** Area under the curve (AUC) represents over all hyperglycemic burden in animals of various groups. It was calculated by the formula reported earlier (Chinnaraju

Docking

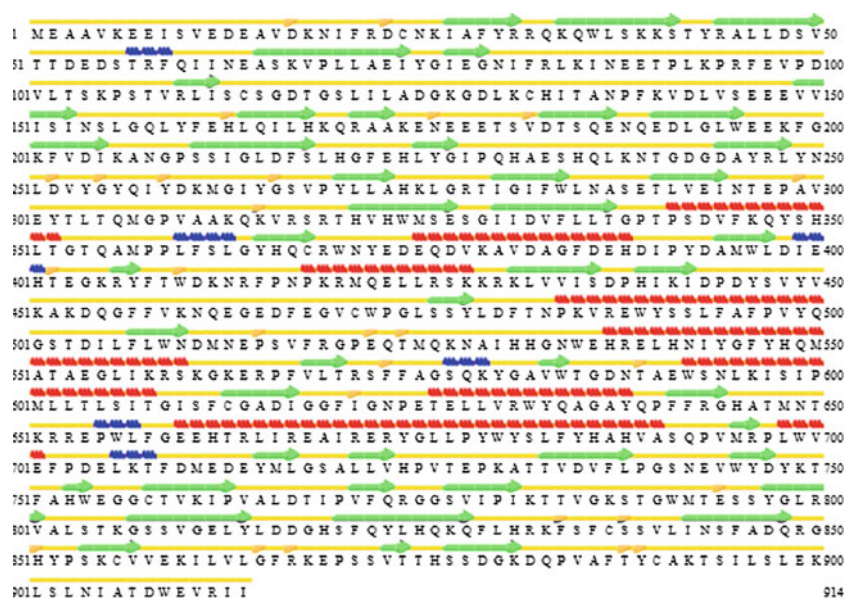
Docking analysis was incorporated in the design and study of inhibitors based on the following observations (Tables 2, 3). In most of the compounds, major interactions of the scaffold rise from the methoxy and hydroxyl groups attached to R^2 , R^3 , and R^4 position of the phenyl ring in both angular and linear chalcones, which corroborated later with the activity profile of compounds **9c** and **11c**. Presence of hydroxyl groups both at R^2 and R^3 tends to cause steric hindrance. Presence of only one hydroxyl group (**9a**) favors better binding. Displacement of furan ring in angular form occupies the active site better than its linear counterpart. In case of linear chalcones, due to the linear position of cyclofuran ring, the inhibitors occupy a linear stretch in the active site. As a result of which catalytic residues like Tyr254 are not reached by the hydroxyl of the cyclofuran. Therefore, on removal of the hydroxyl groups from the phenyl ring of such compounds, H-bond interactions deplete to nil leading to reduction or loss of activity (**10a**, **11a**). Methoxy groups at R^3 and R^4 participate in h-bond formation (**8b**, **8c**) whereas causes steric clash at R^2 .

All the compounds occupied the active site, which is complementary to that of acarbose and showed H-bonding interactions with the residues lining the active site pocket. The calculated binding mode of **8c** is shown in (Fig. 5). Side chain nitrogen of Arg571 forms strong hydrogen bond with carbonyl oxygen of inhibitors and Gln523 and Asp252 form H-bonds as well. The H-bond of hydroxyl group of the benzofuran with the side chain hydroxyl of Tyr254, one of the important catalytic residues, confirms the inhibitory potential of these compounds. These interactions are in conjunction with other glucosidase inhibitor studies (Bharatham *et al.*, 2008; Rodbard *et al.*, 2009).











et al., 2010). one-way ANOVA analysis followed by Bonferroni's multiple comparison tests were applied to find differences between the groups. Values represent mean \pm SD, (standard deviation), $n = 5$. *a* and * $P < 0.001$, *b* $P < 0.01$, and *c* $P < 0.05$

Fig. 3 Secondary structure determination of *Homo sapiens* α -glucosidase (Q8TET4). Homology model with STRIDE



Legend of secondary structure icons:

	H Alpha-Helix		T Turn
	E Extended Configuration (Beta-sheet)		C or " " Coil
	B Isolated Beta Bridge		G 3-10 Helix
	b Isolated Beta Bridge (Type 3 Fig 4,cd)		I Pi-Helix

The compounds show close contacts with many of the active site residues in juxtaposition and opposite side (amino acids 397–399) to the H-bond formers insinuating a probability of interaction under physiological conditions where the protein is flexible and bound to conformational changes.

QSAR

The optimum number of descriptors for the best statistical model describing pIC_{50} μM for the dataset selected according to the breaking point rule for the improvement of R^2 is three comprising of constitutional (1) and quantum-chemical (2). Correlation among the descriptors was checked and then the three descriptors were selected. A number of models were built with varying number and type of descriptors and parameters. The best among the lot was selected. The technique applied for the validation of the proposed three-parameter model was based on the leave-one-out algorithm (LOO). This method gave a squared cross-validated correlation coefficient cross-validate r^2 0.9338, correlation co-efficient (r^2) 0.9889 and $F = 144.31$ (Tables 4, 5). The plot confirms the predictive ability of the model as well as correlates the structure of the inhibitors with activity (Fig. 6). The descriptors envisaged the contribution of groups attached to the B-ring indicating the

importance of this attachment point to be considered during design of lead to improvise activity.

Conclusion

Except compound **8a** all other compounds are being reported utilizing synthetic methodologies for the first time though the natural origin of compounds **8a**, **8b**, and **8c** has already been reported. We report synthesis of compound **6** independently for the first time. Structure and analog based approaches indicate that furanochalcones represent a new class of α -glucosidase inhibitors, and the number and position of hydroxyl substituent in ring B of chalcones are important for inhibition. This is the first report assigning α -glucosidase inhibitory, DPPH free radical scavenging and antihyperglycemic activity to furanochalcones. Most of the in silico observations are in agreement with experimental results.

Experimental section

General

IR spectra were recorded on Nicolet-740 spectrometer with NaCl optics. The ^1H and ^{13}C NMR, spectra were recorded

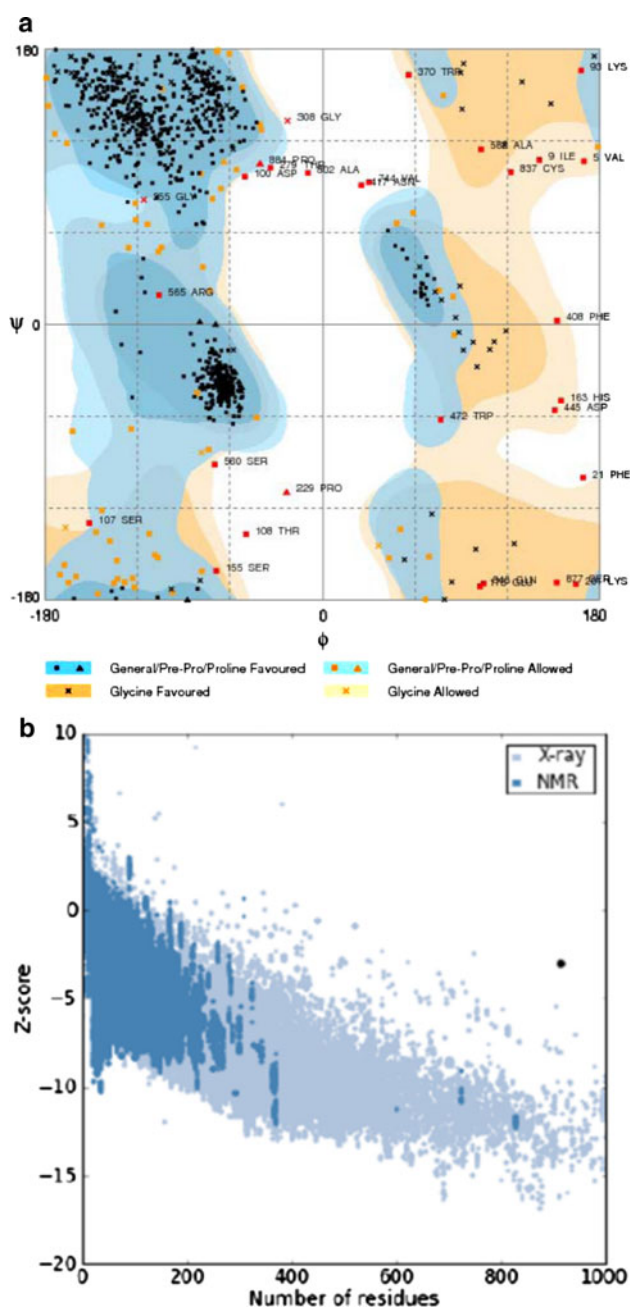


Fig. 4 Validation of homology model of *Homo sapiens* α -glucosidase (Q8TET4)

on a Bruker FT-300 MHz spectrometer at 300 MHz for ^1H and 75 MHz for ^{13}C NMR, respectively, using TMS as internal standard. The chemical shifts were expressed as δ values in parts per million (ppm) and the coupling constants (J) were given in hertz (Hz). HRESIMS were measured on LC-MSD-Trap-SL instrument. Column chromatography was carried out using silica gel 60–120 mesh (Qingdao Marine Chemical, China) and precoated silicagel plates (Merck, 60 F₂₅₄) were used for preparative TLC. Rat intestinal acetone powder as a source of intestinal

α -glucosidase, *p*-nitrophenyl- α -D-glucopyranoside (*p*-NPG) as substrate for enzyme, soluble potato starch, DPPH radical, and EDTA were purchased from Sigma Chemical Co., St Louis, MO, USA. Other chemicals of analytical grade were procured from indigenous manufacturers.

Synthesis of 2-(3,4-bis(benzyloxy)phenyl)-3-hydroxy-4H-furo[2,3-*h*]chromen-4-one (5)

To a solution of furanochalcone (**4**) (0.1 g, 1 eqt) in ethanol (5 ml) was added hydrogen peroxide (30%, 0.25 eqts) in the presence of potassium hydroxide (1 M, 0.5 eqt) at 0°C and stirred for 24 h. After completion of the reaction quenched with 2N HCl, it was extracted with ethyl acetate (50 ml), dried, and concentrated. The product obtained was purified using column chromatography. The fractions eluted at 30% ethyl acetate in petroleum ether contained pure 2-(3,4-bis (benzyloxy)phenyl)-3-hydroxy-4H-furo[2,3-*h*]chromen-4-one as a colorless solid; Yield (0.046 g, 45%); ^1H NMR (300 MHz, CDCl_3): δ 8.13 (d, $J = 8.8$ Hz, 1H), 7.93 (s, 1H), 7.86 (d, $J = 8.4$ Hz, 1H), 7.76 (br s, 1H), 7.60–7.29 (m, 12H, aromatic), 7.08 (br s, 1H), 5.28 (s, 2H, $\text{OCH}_2\text{-Ph}$), 5.30 (s, 2H, $\text{OCH}_2\text{-Ph}$); ^{13}C NMR (75 MHz, CDCl_3): δ 173.0, 158.0, 150.4, 149.9, 148.5, 145.5, 144.0, 137.8, 137.0, 136.7, 128.6 (2C), 128.5 (2C), 127.9, 127.8, 127.3 (2C), 127.1 (2C), 124.1, 121.5, 121.4, 116.9, 115.9, 114.2, 114.0, 110.0, 104.1, 71.4, 70.9; ESI-MS m/z 491.0 [$M + \text{H}$] $^+$.

Synthesis of 3,3',4'-trihydroxy-4H-furo[2,3-*h*]chromen-4-one (6) (Rao et al., 2009)

To a solution of 2-(3,4-bis (benzyloxy) phenyl)-3-hydroxy-4H-furo[2,3-*h*]chromen-4-one (0.1 g, 1eqt) in dry DCM was added TiCl_4 (0.066 ml, 3 eqts) in dry DCM (2 ml) at -10°C under nitrogen atmosphere stir for 15 min. After the completion of the reaction, the reaction mixture was quenched with 2 N HCl and extracted with ethyl acetate (50 ml), dried, and concentrated. The yellow product obtained was purified using column chromatography. The fractions eluted at 25% methanol in chloroform contained pure 3,3',4'-trihydroxy-4H-furo[2,3-*h*]chromen-4-one (0.040 g, Yield 64%).

General experimental procedure for the synthesis of angular furanochalcones (8a–8g)

The acetophenone derivative (**1**) (50 mg, 0.284 mmol) was condensed with various substituted benzaldehydes (**7a–7g**) (0.284 mmol), respectively, in the presence of aq. KOH (60%, 1 ml) in anhydrous ethanol (5 ml). The reaction mixture was stirred at room temperature for 24 h and poured into water (20 ml). After neutralization with

Table 2 Scoring component of Glucosidase (Homology model)–furanochalcones interaction in Glide 4.5

Sr. no.	Molecule	vdW	Coul	Lipo	HBond	Metal	Rewards	RotB	Site	GScore	Glide rank
1	8(a)	-34.2	-15.6	-0.6	-0.5	0	-1.3	0.6	0	-5.83	10
2	8(b)	-30.9	-18.2	-0.7	-0.6	0	-1.3	0.6	0	-6.38	2
3	8(c)	-23.7	-20.7	-0.8	-0.6	0	-1.5	0.6	0	-6.63	1
4	8(d)	-29.9	-17.5	-0.7	0	0	-1.4	0.4	0	-5.96	8
5	9(a)	-32	-17.5	-0.8	-0.6	0	-1.3	0.6	0	-6.35	3
6	9(b)	-25.4	-18.8	-0.4	-0.6	0	-1.3	0.6	-0.1	-5.88	9
7	9(c)	-29.2	-17.5	-0.5	-0.4	0	-1.6	0.6	0	-5.96	7
8	11(a)	-33.7	-16.9	-0.7	-0.6	0	-1.3	0.6	0	-6.28	6
9	11(b)	-19.6	-23.5	-0.3	-0.1	0	-1.3	0.5	0	-5.74	14
10	11(c)	-32.1	-17.6	-0.8	-0.6	0	-1.3	0.6	0	-6.32	4
11	11(d)	-32.8	-17.5	-0.7	-0.6	0	-1.3	0.6	0	-6.32	5
12	12(a)	-33.7	-14.6	-0.3	-0.8	0	-1.4	0.6	0	-5.8	11
13	12(b)	-35.1	-12.6	-0.7	-0.5	0	-1.6	0.6	0	-5.76	13
14	12(c)	-31.3	-14.6	-0.6	-0.6	0	-1.3	0.6	-0.1	-5.79	12

Table 3 Scoring component of α -glucosidase (Homology model)–furanochalcones interaction in GOLD 3.2

Sr. no.	Molecule	S (hb_int)	S (hb_ext)	S (int)*	S (vdw_ext)	Fitness	GOLD rank
1	8(a)	0	2	-30.42	42.74	30.34	10
2	8(b)	0	0.44	-36.14	49.12	31.84	2
3	8(c)	0	0	0	23.25	31.97	1
4	8(d)	0	1.06	-21.37	37.48	31.22	7
5	9(a)	0	0	0	23.05	31.69	4
6	9(b)	0	0	-19.9	36.96	30.92	8
7	9(c)	0	0	-1.12	23.2	30.79	9
8	11(a)	0	2.96	-26.22	41.77	31.26	6
9	11(b)	0	2.54	-44.58	52.18	29.7	13
10	11(c)	0	0	0	23	31.62	5
11	11(d)	0	0	0	23.14	31.82	3
12	12(a)	0	0	-40.3	51.17	30.07	12
13	12(b)	0	0.53	-24.32	37.41	27.65	14
14	12(c)	0	0	0	21.93	30.16	11

hydrochloric acid (10% w/v), ethanol was evaporated, and extracted thrice with ethyl acetate (50 ml), and the combined organic phases were concentrated to yield crude product. The crude product was subjected to column chromatography to yield pure products (**8a–8g**), respectively (Scheme 2).

(*E*)-1-(4-hydroxybenzofuran-5-yl)-3-phenylprop-2-en-1-one (**8a**) (Saxena et al., 1987)

Yellow amorphous powder; Yield (53 mg, 70%); $R_f = 0.62$ (Hexane/Ethyl acetate, 9:1); mp: 108–109°C; IR (KBr) ν_{\max} : 3456, 1645, 1595, 1490, 1472, 1446, 1420, 1360, 1334, 1315, 1256, 1215, 1150, 1071, 965, 815 cm^{-1} ; ^1H NMR (300 MHz, CDCl_3): δ 13.90 (s, 1H, Chelated

OH), 7.90 (d, $J = 15.4$ Hz, 1H), 7.82 (d, $J = 8.8$ Hz, 1H), 7.66 (d, $J = 15.4$ Hz, 1H), 7.64 (m, 2H), 7.55 (d, $J = 2.2$ Hz, 1H), 7.41 (m, 3H), 7.04 (d, $J = 8.8$ Hz, 1H), 7.01 (dd, $J = 2.2, 0.9$ Hz, 1H); ^{13}C NMR (75 MHz, CDCl_3): δ 193.2, 160.2, 159.7, 144.8, 144.4, 134.6, 130.7, 128.9 (2C), 128.5 (2C), 128.2, 125.9, 120.6, 114.3, 105.0, 103.7; HRESIMS: m/z [$M + \text{H}$] $^+$ calcd for $\text{C}_{17}\text{H}_{13}\text{O}_3$: 265.0859, found: 265.0868.

(*E*)-1-(4-hydroxybenzofuran-5-yl)-3-(4-methoxyphenyl)prop-2-en-1-one (**8b**) (Talapatra et al., 1982)

Yellow amorphous powder; Yield (70 mg, 85%); $R_f = 0.60$ (Hexane/Ethyl acetate, 8:2); mp: 140–141°C; IR

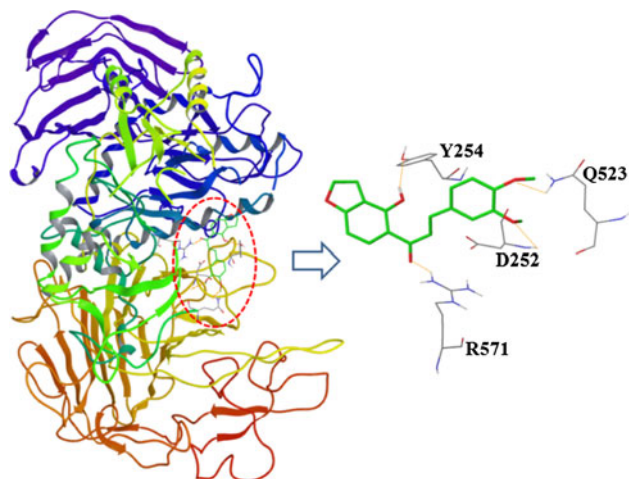


Fig. 5 Binding mode of comp-10 in the active site of *Homo sapiens* α -glucosidase (Q8TET4) homology model depicting the H-bond formers (Tyr254 OH:H23; Arg571 NH1:O4; Gln523 NH2:35; Asp252 NH:O31)

(KBr) ν_{\max} : 3426, 1630, 1595, 1508, 1467, 1360, 1287, 1242, 1160, 1090, 1040, 820, 785 and 730 cm^{-1} ; ^1H NMR (300 MHz, CDCl_3): δ 14.12 (s, 1H, Chelated OH), 7.92 (d, $J = 15.2$ Hz, 1H), 7.86 (d, $J = 8.8$ Hz, 1H), 7.64 (d, $J = 8.8$ Hz, 1H), 7.58 (s, 1H), 7.57 (d, $J = 15.2$ Hz, 1H), 7.08 (d, $J = 8.8$ Hz, 2H), 7.03 (d, $J = 2.0$ Hz, 1H), 6.96 (d, $J = 8.8$ Hz, 2H), 3.87 (s, 3H, OMe); ^{13}C NMR (75 MHz, CDCl_3): δ 193.2, 161.8, 160.1, 159.6, 144.6, 144.3, 130.3 (2C), 128.8, 127.3, 125.8, 124.5, 117.9, 114.3 (2C), 104.9, 103.4, 55.3; HRESIMS: m/z $[M + \text{H}]^+$ calcd for $\text{C}_{18}\text{H}_{15}\text{O}_4$: 295.0965, found: 295.0970.

(*E*)-3-(3,4-dimethoxyphenyl)-1-(4-hydroxybenzofuran-5-yl)prop-2-en-1-one (**8c**) (Sritularak and Likhitwitayawuid, 2006)

Yellow solid; Yield (82 mg, 90%); $R_f = 0.52$ (Hexane/Acetone, 8:2); mp: 164–165°C; IR (KBr) ν_{\max} : 3423, 1635,

Table 5 Details of models built with Heuristic method by 2D-QSAR CODESSA2.7.1 for α -human glucosidase inhibitors with Heuristic method

Model no.	R^2	F	No. of descriptors
1	0.99	144.31	3
2	0.98	86.14	3
3	0.98	70.45	3
4	0.97	59.40	3
5	0.97	55.03	3
6	0.97	54.28	3
7	0.97	52.83	3
8	0.97	51.07	3
9	0.960	50.76	3
10	0.95	51.65	3

1565, 1461, 1398, 1281, 980, 759 cm^{-1} ; ^1H NMR (300 MHz, CDCl_3): δ 14.02 (s, 1H, Chelated OH), 7.87 (d, $J = 15.2$ Hz, 1H), 7.82 (d, $J = 8.8$ Hz, 1H), 7.56 (d, $J = 2.0$ Hz, 1H), 7.49 (d, $J = 15.2$ Hz, 1H), 7.26 (br s, 1H), 7.23 (d, $J = 1.7$ Hz, 1H), 7.15 (d, $J = 1.7$ Hz, 1H), 7.04 (d, $J = 8.8$ Hz, 1H), 7.01 (d, $J = 2.0, 0.7$ Hz, 1H), 6.88 (d, $J = 8.4$ Hz, 1H), 3.96 (s, 3H, OMe), 3.93 (s, 3H, OMe); ^{13}C NMR (75 MHz, CDCl_3): δ 193.1, 160.1, 159.6, 151.6, 149.2, 114.9, 114.3, 127.6, 125.8, 123.4, 118.1, 117.6, 114.4, 111.0, 110.1, 104.9, 103.5, 55.9 (2C); HRESIMS: m/z $[M + \text{H}]^+$ calcd for $\text{C}_{19}\text{H}_{17}\text{O}_5$: 325.1071, found: 325.1082.

(*E*)-1-(4-hydroxybenzofuran-5-yl)-3-(2,3,4-trimethoxyphenyl)prop-2-en-1-one (**8d**)

Yellow solid; Yield (80 mg, 79%); $R_f = 0.55$ (Hexane/Acetone, 7:3); mp: 171–172°C; IR (KBr) ν_{\max} : 3430, 1630, 1603, 1565, 1458, 1395, 1283, 1206, 1127, 980, 901, 840, 802, 761 cm^{-1} ; ^1H NMR (300 MHz, CDCl_3): δ 14.15 (s, 1H, Chelated OH), 8.11 (d, $J = 15.4$ Hz, 1H), 7.84 (d, $J = 8.8$ Hz, 1H), 7.73 (d, $J = 15.4$ Hz, 1H), 7.58 (d, $J = 2.0$ Hz, 1H), 7.42 (d, $J = 8.6$ Hz, 1H), 7.07 (d,

Table 4 Equation for the prediction of biological activity generated by 2D-QSAR CODESSA2.7.1 for α -human glucosidase inhibitors with Heuristic method (three descriptors)

X	DX	t Test	Descriptors	Type	
0	1.7699e+01	8.2387e+00	21.4823	Intercept	
1	9.8912e+02	5.5205e+01	17.9171	Avg 1-electron react. index for a O atom	Constitutional
2	1.5592e+00	1.0892e-01	14.3145	HOMO-1 energy	Quantum-chemical
3	9.8023e+00	2.2465e+00	4.3633	RNCG Relative negative charge (QMNEG/QTMINUS) [quantum-chemical PC]	Quantum-chemical

Test Set: 11(d), 12(c) $R^2 = 0.9886$; $F = 144.31$; $s^2 = 0.0012$; cross-validated $R^2 = 0.9338$

Biological activity = (17.699) + [(989.12) * (Avg 1-electron react. index for a O atom)] + [(1.5592) * (HOMO-1 energy)] + [(9.8023) * (RNCG Relative negative charge (QMNEG/QTMINUS) [Quantum-Chemical PC])]

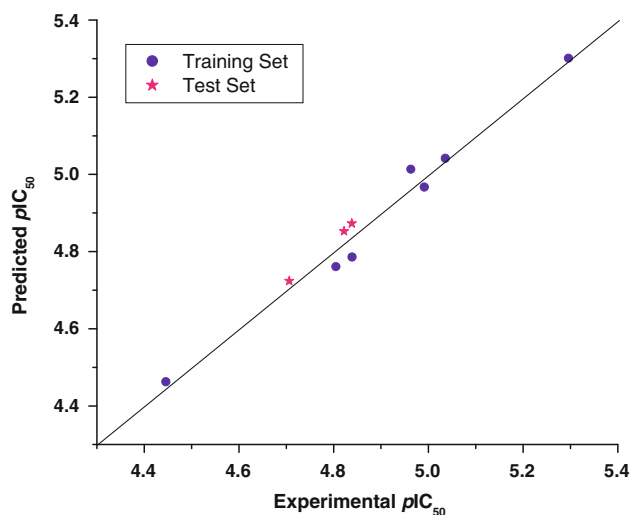


Fig. 6 Calculated versus experimental pIC_{50} (μM) based on the three-parameter correlation equation (with a $R^2 = 0.9889$) from 2D-QSAR model for the entire data set for α -human glucosidase inhibitors

$J = 8.8$ Hz, 1H), 7.02 (d, $J = 1.3$ Hz, 1H), 6.70 (d, $J = 8.6$ Hz, 1H), 3.99 (s, 3H, OMe), 3.93 (s, 3H, OMe), 3.90 (s, 3H, OMe); ^{13}C NMR (75 MHz, $CDCl_3$): δ 193.5, 160.0, 159.5, 155.9, 153.8, 144.2, 142.3, 140.1, 125.8, 124.1, 121.6, 119.4, 117.5, 114.4, 107.5, 104.8, 103.4, 61.3, 60.7, 55.9; HRESIMS: m/z $[M + H]^+$ calcd for $C_{20}H_{19}O_6$: 355.1176, found: 355.1194.

(E)-3-(4-(benzyloxy)phenyl)-1-(4-hydroxybenzofuran-5-yl)prop-2-en-1-one (**8e**)

Yellow solid; Yield (77 mg, 74%); $R_f = 0.59$ (Hexane/Ethyl acetate, 9:1); mp: 120–121°C; 1H NMR (300 MHz, $CDCl_3$): δ 14.11 (s, 1H, Chelated OH), 7.91 (d, $J = 15.4$ Hz, 1H), 7.84 (d, $J = 8.8$ Hz, 1H), 7.63 (d, $J = 8.4$ Hz, 2H), 7.60–7.52 (m, 2H), 7.48–7.30 (m, 5H), 7.08 (d, $J = 8.8$ Hz, 1H), 7.03 (m, 3H), 5.13 (s, 2H, OCH_2Ph); ^{13}C NMR (75 MHz, $CDCl_3$): δ 193.3, 161.0, 160.2, 159.7, 144.6, 144.3, 136.3, 130.4 (2C), 128.6 (2C), 128.1, 127.6, 127.4 (2C), 125.9, 118.2, 117.6, 115.3 (2C), 114.4, 105.0, 103.6, 70.1; ESI-MS m/z 371.0 $[M + H]^+$.

(E)-3-(4-(benzyloxy)-3-methoxyphenyl)-1-(4-hydroxybenzofuran-5-yl)prop-2-en-1-one (**8f**)

Yellow amorphous powder; Yield (82 mg, 72%); $R_f = 0.54$ (Hexane/Ethylacetate, 8.5:1.5); mp: 130–131°C; 1H NMR (300 MHz, $CDCl_3$): δ 14.10 (s, 1H, Chelated OH), 7.94–7.79 (m, 2H), 7.57(d, $J = 1.7$ Hz, 1H), 7.52 (d, $J = 15.4$ Hz, 1H), 7.47–7.28 (m, 5H), 7.19 (br s, 2H), 7.07 (d, $J = 8.6$ Hz, 1H), 7.02 (br s, 1H), 6.92 (d, $J = 8.6$ Hz, 1H), 5.21 (s, 2H, OCH_2Ph), 3.97 (s, 3H, OMe); ^{13}C NMR

(75 MHz, $CDCl_3$): δ 193.2, 160.1, 159.6, 150.7, 149.7, 144.9, 144.3, 136.4, 128.6 (2C), 128.0 (2C), 127.1 (2C), 125.9, 123.1, 118.3, 117.7, 114.4, 113.3, 110.8, 105.0, 103.5, 70.8, 56.0; ESI-MS m/z 401.0 $[M + H]^+$.

(E)-3-(3,4-bis(benzyloxy)phenyl)-1-(4-hydroxybenzofuran-5-yl)prop-2-en-1-one (**8g**) (Rao et al., 2009)

Yellow amorphous powder; Yield (101 mg, 75%); $R_f = 0.58$ (Hexane/Ethyl acetate, 8.5:1.5); mp: 171–172°C; 1H NMR (300 MHz, $CDCl_3$): δ 13.9 (s, 1H, Chelated OH), 7.8 (d, $J = 8.8$ Hz, 1H), 7.76 (d, $J = 8.8$ Hz, 1H), 7.55 (d, $J = 2.2$ Hz, 1H), 7.49–7.26 (m, 12H), 7.24 (d, $J = 9.4$ Hz, 1H), 7.02 (d, $J = 8.8$ Hz, 1H), 7.0 (d, $J = 8.4$ Hz, 1H), 6.92 (d, $J = 8.4$ Hz, 1H), 5.20 (s, 4H); ^{13}C NMR (75 MHz, $CDCl_3$): δ 192.8, 160.4, 159.6, 151.5, 149.03, 145.1, 144.7, 144.1, 136.9, 136.6, 128.5, 128.0, 127.3, 127.1, 125.8, 123.7, 118.4, 117.8, 114.4, 114.3, 114.1, 105.2, 103.4, 71.4, 70.8; ESI-MS m/z 477.0 $[M + H]^+$.

General experimental procedure for the synthesis of angular hydroxy furanochalcones (9a–9c)

Benzyl-protected furanochalcones (**8e–8g**) were debenzylated using $TiCl_4$ in dry DCM at $-10^\circ C$ for 15 min under nitrogen atmosphere. After completion (TLC), the reaction mixture was neutralized with aq. HCl, it was extracted thrice with ethyl acetate (50 ml) and dried over sodium sulfate. The combined organic phases were concentrated to yield crude product, it was subjected to column chromatography to afford angular hydroxy furanochalcones (**9a–9c**) (Scheme 2).

(E)-1-(4-hydroxybenzofuran-5-yl)-3-(4-hydroxyphenyl)prop-2-en-1-one (**9a**)

Yellow amorphous powder; Yield (24.5 mg, 68%); $R_f = 0.55$ (Hexane/Acetone, 8.5:1.5); mp: 152–153°C; IR (KBr) ν_{max} : 3221, 1634, 1594, 1511, 1463, 1365, 1215, 1161, 1098, 978, 822, 735 cm^{-1} ; 1H NMR (300 MHz, $CDCl_3$): δ 14.35 (s, 1H, Chelated OH), 9.16 (br s, 1H, Chelated OH), 8.22 (d, $J = 8.8$ Hz, 1H), 7.98–7.85 (m, 3H), 7.80 (d, $J = 8.6$ Hz, 2H), 7.16 (dd, $J = 8.8, 0.7$ Hz, 1H), 7.06 (dd, $J = 2.0, 0.7$ Hz, 1H), 6.96 (d, $J = 8.6$ Hz, 2H); ^{13}C NMR (75 MHz, ACETONE- d_6): δ 192.0, 162.4, 161.8, 161.4, 147.2, 146.9, 133.7, 133.0 (2C), 128.6, 128.2, 119.1, 117.8 (2C), 117.6, 106.4, 105.1; ESI-MS m/z 280.1 $[M + H]^+$.

(E)-3-(4-hydroxy-3-methoxyphenyl)-1-(4-hydroxybenzofuran-5-yl)prop-2-en-1-one (**9b**)

Yellow amorphous powder; Yield (23 mg, 60%); $R_f = 0.40$ (Hexane/Acetone, 8:2); mp: 160–161°C; IR

(KBr) ν_{\max} : 3228, 1638, 1599, 1518, 1469, 1368, 1218, 1166, 1096, 974, 828, 732 cm^{-1} ; ^1H NMR (300 MHz, CDCl_3 + ACETONE- d_6): δ 9.78 (br s, 2H, Chelated OH), 7.95 (d, $J = 8.8$ Hz, 1H), 7.86 (d, $J = 15.2$ Hz, 1H), 7.67–7.51 (m, 2H), 7.39–7.20 (m, 3H), 7.05 (d, $J = 8.8$ Hz, 1H), 6.98 (d, $J = 8.3$ Hz, 1H), 6.91 (d, $J = 8.3$ Hz, 1H), 3.95 (s, 3H); ^{13}C NMR (75 MHz, CDCl_3 + ACETONE- d_6): δ 193.3, 162.0, 159.5, 148.6, 146.1, 145.5, 123.5, 122.7, 120.2, 119.5, 117.8, 114.9, 110.3, 108.7, 107.0, 106.6, 100.0, 56.0; HRESIMS: m/z $[M + \text{H}]^+$ calcd for $\text{C}_{18}\text{H}_{15}\text{O}_5$: 311.0914, found: 311.0929.

(E)-3-(3,4-dihydroxyphenyl)-1-(4-hydroxybenzofuran-5-yl)prop-2-en-1-one (**9c**)

Yellow amorphous powder; Yield (21 mg, 68%); $R_f = 0.52$ (Hexane/Acetone, 6:4); mp: 216–217°C; IR (KBr) ν_{\max} : 3410, 1678, 1595, 1447, 1361, 1292, 1164, 831, 732 cm^{-1} ; ^1H NMR (300 MHz, CDCl_3 + ACETONE- d_6): δ 13.20 (br s, 1H, Chelated OH), 9.71 (s, 2H, chelated OH), 8.22 (s, 1H), 7.80 (d, $J = 15.2$ Hz, 1H), 7.58–7.52 (m, 2H), 7.43 (br s, 1H), 7.36 (br s, 1H), 7.29 (d, $J = 8.2$ Hz, 1H), 7.02 (s, 1H), 6.76 (br s, 1H); ^{13}C NMR (75 MHz, CDCl_3 + ACETONE- d_6): δ 193.2, 160.3, 159.8, 151.8, 149.4, 115.1, 114.5, 127.8, 126.0, 123.6, 118.3, 117.8, 114.6, 111.2, 110.3, 105.0, 103.7; HRESIMS: m/z $[M-\text{H}]^+$ calcd for $\text{C}_{17}\text{H}_{11}\text{O}_5$: 295.0612, found: 295.0597.

General experimental procedure for the synthesis of linear furanochalcones (10a–10g)

The acetophenone derivative (**2**) (50 mg, 0.284 mmol) was condensed with various substituted benzaldehydes (0.284 mmol) (**7a–7g**), respectively, in the presence of aq. KOH (60%, 1 ml) in anhydrous ethanol (5 ml). The reaction mixture was stirred at room temperature for 24 h and poured into water (20 ml). After neutralization with hydrochloric acid (10% w/v), ethanol was evaporated, and extracted thrice with ethyl acetate (50 ml). The combined organic phases were concentrated to yield crude products. The crude products were subjected to column chromatography to yield pure products (**10a–10g**), respectively (Scheme 3).

(E)-1-(6-hydroxybenzofuran-5-yl)-3-phenylprop-2-en-1-one (**10a**)

Yellow amorphous powder; Yield (60 mg, 80%); $R_f = 0.52$ (Hexane/Ethyl acetate, 9:1); mp: 121–122°C; IR (KBr) ν_{\max} : 3339, 1741, 1669, 1593, 1510, 1463, 1430, 1383, 1267, 1155, 1096, 1031, 859, 817 cm^{-1} ; ^1H NMR (300 MHz, CDCl_3): δ 12.86 (s, 1H, Chelated OH), 8.16 (s, 1H), 7.93 (d, $J = 15.4$ Hz, 1H), 7.71 (d, $J = 15.4$ Hz, 1H),

7.67 (m, 2H), 7.55 (d, $J = 2.2$ Hz, 1H), 7.42 (m, 3H), 7.06 (s, 1H), 6.72 (dd, $J = 2.0, 0.7$ Hz, 1H); ^{13}C NMR (75 MHz, CDCl_3): δ 193.4, 169.4, 162.1, 145.6, 145.1, 134.6, 130.8, 130.4, 129.0 (2C), 128.6 (2C), 128.3, 122.9, 120.4, 106.5, 100.0; HRESIMS: m/z $[M + \text{H}]^+$ calcd for $\text{C}_{17}\text{H}_{13}\text{O}_3$: 265.0859, found: 265.0870.

(E)-1-(6-hydroxybenzofuran-5-yl)-3-(4-methoxyphenyl)prop-2-en-1-one (**10b**)

Yellow amorphous powder; Yield (83 mg, 92%); $R_f = 0.50$ (Hexane/Ethyl acetate, 8:2); mp: 146–147°C; IR (KBr) ν_{\max} : 3432, 1636, 1592, 1505, 1465, 1363, 1285, 1241, 1160, 1090, 1040, 822, 786 and 730 cm^{-1} ; ^1H NMR (300 MHz, CDCl_3): δ 13.11 (s, 1H, Chelated OH), 8.19 (s, 1H), 7.93 (d, $J = 15.4$ Hz, 1H), 7.66 (d, $J = 8.8$ Hz, 2H), 7.61 (d, $J = 15.4$ Hz, 1H), 7.57 (d, $J = 2.2$ Hz, 1H), 7.09 (s, 1H), 6.97 (d, $J = 8.8$ Hz, 2H), 6.76 (dd, $J = 2.0, 0.7$ Hz, 1H), 3.88 (s, 3H, OMe); ^{13}C NMR (75 MHz, CDCl_3): δ 193.3, 162.0, 161.9, 159.3, 145.5, 145.0, 130.4 (2C), 128.9, 127.3, 122.8, 120.0, 117.8, 114.4 (2C), 106.6, 99.9, 55.3; HRESIMS: m/z $[M + \text{H}]^+$ calcd for $\text{C}_{18}\text{H}_{15}\text{O}_4$: 295.0965, found: 295.0971.

(E)-3-(3,4-dimethoxyphenyl)-1-(6-hydroxybenzofuran-5-yl)prop-2-en-1-one (**10c**)

Yellow amorphous powder; Yield (80 mg, 91%); $R_f = 0.40$ (Hexane/Acetone, 8:2); mp: 171°C; IR (KBr) ν_{\max} : 3428, 1625, 1569, 1460, 1398, 1280, 980, 898, 759 cm^{-1} ; ^1H NMR (300 MHz, CDCl_3): δ 13.07 (s, 1H, Chelated OH), 8.19 (s, 1H), 7.90 (d, $J = 15.2$ Hz, 1H), 7.59 (d, $J = 2.2$ Hz, 1H), 7.56 (d, $J = 15.2$ Hz, 1H), 7.29 (dd, $J = 8.4, 1.8$ Hz, 1H), 7.20 (d, $J = 1.8$ Hz, 1H), 7.08 (s, 1H), 6.92 (d, $J = 8.4$ Hz, 1H), 6.76 (dd, $J = 2.0, 0.7$ Hz, 1H), 3.98 (s, 3H, OMe), 3.95 (s, 3H, OMe); ^{13}C NMR (75 MHz, CDCl_3): δ 193.2, 162.0, 159.4, 151.6, 149.2, 145.5, 145.3, 143.4, 127.5, 123.3, 122.8, 119.9, 118.0, 117.1, 110.9, 110.1, 106.6, 99.8, 56.0; HRESIMS: m/z $[M + \text{H}]^+$ calcd for $\text{C}_{19}\text{H}_{17}\text{O}_5$: 325.1071, found: 325.1086.

(E)-1-(6-hydroxybenzofuran-5-yl)-3-(2,4,5-trimethoxyphenyl)prop-2-en-1-one (**10d**)

Yellow amorphous powder; Yield (85 mg, 86%); $R_f = 0.45$ (Hexane/Acetone, 7:3); mp: 179–180°C; IR (KBr) ν_{\max} : 3432, 1633, 1606, 1568, 1461, 1398, 1286, 1209, 1130, 981, 901, 843, 804, 761 cm^{-1} ; ^1H NMR (300 MHz, CDCl_3): δ 13.15 (s, 1H, Chelated OH), 8.18 (d, $J = 15.2$ Hz, 1H), 8.13 (s, 1H), 7.60 (d, $J = 15.2$ Hz, 1H), 7.52 (d, $J = 2.0$ Hz, 1H), 7.11 (s, 1H), 7.04 (s, 1H), 6.72 (dd, $J = 2.0, 0.7$ Hz, 1H), 6.49 (s, 1H), 3.95 (s, 3H, OMe), 3.94 (s, 3H, OMe), 3.92 (s, 3H, OMe); ^{13}C NMR (75 MHz,

CDCl_3): δ 193.6, 162.0, 159.2, 154.9, 152.8, 145.3, 140.5, 138.2, 125.1, 122.7, 119.8, 117.9, 115.1, 111.6, 106.6, 99.7, 96.6, 56.5, 56.2, 55.9; HRESIMS: m/z $[M + H]^+$ calcd for $\text{C}_{20}\text{H}_{19}\text{O}_6$: 355.1176, found: 355.1194.

(*E*)-3-(4-(benzyloxy)phenyl)-1-(6-hydroxybenzofuran-5-yl)prop-2-en-1-one (**10e**)

Yellow amorphous powder; Yield (84 mg, 81%); R_f = 0.55 (Hexane/Ethyl acetate, 9:1); mp: 160–161°C; ^1H NMR (300 MHz, CDCl_3): δ 13.08 (s, 1H, Chelated OH), 8.18 (br s, 1H), 7.92 (d, J = 15.4 Hz, 1H), 7.70–7.61 (m, 3H), 7.59–7.53 (m, 1H), 7.50–7.31 (m, 5H), 7.13–6.98 (m, 3H), 6.75 (br s, 1H), 5.14 ppm (s, 2H, OCH_2Ph); ^{13}C NMR (75 MHz, CDCl_3): δ 193.4, 162.1, 161.1, 159.4, 145.5, 145.0, 136.3, 130.4 (2C), 128.6 (2C), 128.2, 127.6, 127.4 (2C), 122.7, 120.0, 118.0, 117.4, 115.3 (2C), 106.6, 99.9, 70.1; ESI-MS m/z 371.3 $[M + H]^+$.

(*E*)-3-(4-(benzyloxy)-3-methoxyphenyl)-1-(6-hydroxybenzofuran-5-yl)prop-2-en-1-one (**10f**) (Anuradha, et al., 2006)

Yellow amorphous powder; Yield (85 mg, 75%); R_f = 0.50 (Hexane/Ethyl acetate, 8.5:1.5); mp: 131–132°C; ^1H NMR (300 MHz, CDCl_3): δ 12.94 (s, 1H, Chelated OH), 8.14 (s, 1H), 7.85 (d, J = 15.4 Hz, 1H), 7.54 (d, J = 2 Hz, 1H), 7.47–7.30 (m, 7H), 7.18 (d, J = 2 Hz, 1H), 7.05 (s, 1H), 6.90 (d, J = 15.4 Hz, 1H), 6.72 (d, J = 2 Hz, 1H), 5.19 (s, 2H, OCH_2Ph), 3.98 (s, 3H, OMe); ESI-MS m/z 401.0 $[M + H]^+$.

(*E*)-3-(3,4-bis(benzyloxy)phenyl)-1-(6-hydroxybenzofuran-5-yl)prop-2-en-1-one (**10g**) (Anuradha, et al., 2006)

Yellow amorphous powder; Yield (106 mg, 79%); R_f = 0.54 (Hexane/Ethyl acetate, 8:2); mp: 175–176°C; ^1H NMR (300 MHz, CDCl_3): δ 8.18 (s, 1H), 7.80 (d, J = 15.4 Hz, 1H), 7.58 (d, J = 2.0 Hz, 1H), 7.42–7.30 (m, 13H), 7.12 (d, J = 2.0 Hz, 1H), 7.02 (s, 1H), 6.90 (d, J = 8 Hz, 1H), 6.70 (d, J = 2.0 Hz, 1H), 5.28 (s, 2H, OCH_2Ph), 5.23 (s, 2H, OCH_2Ph); ESI-MS m/z 477.0 $[M + H]^+$.

General experimental procedure for the synthesis of linear hydroxy furano chalcones (**11a–11c**)

Benzyl protected furanochalcones (**10e–10g**) were debenzylated using TiCl_4 in dry DCM at -10°C for 15 min under nitrogen atmosphere. After completion (TLC), the reaction mixture was neutralized with aq. HCl, it was extracted thrice with ethyl acetate (50 ml) and dried over sodium sulfate. The combined organic phases were

concentrated to yield crude product. The crude product was subjected to column chromatography to afford angular and linear hydroxy furanochalcones (**11a–11c**, respectively) (Scheme 3).

(*E*)-1-(6-hydroxybenzofuran-5-yl)-3-(4-hydroxyphenyl)prop-2-en-1-one (**11a**)

Yellow amorphous powder; Yield (25 mg, 70%); R_f = 0.45 (Hexane/Acetone, 8.5:1.5); mp: 160–161°C; IR (KBr) ν_{max} : 3224, 1630, 1598, 1510, 1461, 1360, 1213, 1160, 1094, 972, 820, 730 cm^{-1} ; ^1H NMR (300 MHz, CDCl_3): δ 13.18 (s, 1H, Chelated OH), 8.19 (s, 1H), 8.01 (s, 1H), 7.89 (d, J = 15.2 Hz, 1H), 7.57 (d, J = 15.2 Hz, 1H), 7.55–7.52 (m, 3H), 6.98–6.70 (m, 3H), 6.75 (dd, J = 2.0, 0.7 Hz, 1H); ^{13}C NMR (75 MHz, CDCl_3): δ 193.4, 175.6, 162.7, 161.9, 160.1, 159.3, 145.6, 145.4, 130.6, 126.1, 122.7, 120.0, 117.3, 116.8, 116.2, 106.6, 99.7; ESI-MS m/z 281.0 $[M + H]^+$.

(*E*)-3-(4-hydroxy-3-methoxyphenyl)-1-(6-hydroxybenzofuran-5-yl)prop-2-en-1-one (**11b**)

Yellow amorphous powder; Yield (25 mg, 65%); R_f = 0.30 (Hexane/Acetone, 8:2); mp: 166–167°C; IR (KBr) ν_{max} : 3230, 1640, 1596, 1515, 1467, 1363, 1215, 1167, 1098, 978, 829, 736 cm^{-1} ; ^1H NMR (300 MHz, $\text{CDCl}_3 + \text{ACETONE-d}_6$): δ 13.09 (s, 1H, Chelated OH), 8.20 (s, 1H), 7.90 (d, J = 15.2 Hz, 1H), 7.57 (d, J = 2.0 Hz, 1H), 7.58 (d, J = 15.2 Hz, 1H), 6.99 (d, J = 8.3 Hz, 1H), 6.76 (dd, J = 2.0, 0.7 Hz, 1H), 5.90 (s, 1H), 4.01 (s, 3H); ^{13}C NMR (75 MHz, $\text{CDCl}_3 + \text{ACETONE-d}_6$): δ 189.1, 151.7, 147.0, 144.6, 143.7, 128.5, 125.4, 123.3, 116.5, 114.3, 113.9 (2C), 110.0, 108.7 (2C), 103.8, 102.2, 54.5; HRESIMS: m/z $[M + H]^+$ calcd for $\text{C}_{18}\text{H}_{15}\text{O}_5$: 311.0914, found: 311.0929.

(*E*)-3-(3,4-dihydroxyphenyl)-1-(6-hydroxybenzofuran-5-yl)prop-2-en-1-one (**11c**)

Yellow amorphous powder; Yield (22 mg, 54%); R_f = 0.42 (Hexane/Acetone, 6:4); mp: 232–233°C; IR (KBr) ν_{max} : 3409, 1677, 1594, 1446, 1360, 1291, 1163, 830, 732 cm^{-1} ; ^1H NMR (300 MHz, $\text{CDCl}_3 + \text{ACETONE-d}_6$): δ 13.20 (br s, 1H, Chelated OH), 9.71 (s, 2H, Phenolic OH), 8.22 (s, 1H), 7.80 (d, J = 15.2 Hz, 1H), 7.58–7.52 (m, 2H), 7.43 (br s, 1H), 7.36 (br s, 1H), 7.29 (d, J = 8.2 Hz, 1H), 7.02 (s, 1H), 6.76 (br s, 1H); ^{13}C NMR (75 MHz, $\text{CDCl}_3 + \text{ACETONE-d}_6$): δ 193.5, 161.8, 151.4, 148.0, 145.8, 145.4, 145.0, 144.8, 129.4, 125.4, 123.1, 117.3, 115.6, 115.5, 114.5, 106.8, 99.5; HRESIMS: m/z $[M - H]^+$ calcd for $\text{C}_{17}\text{H}_{11}\text{O}_5$: 295.0612, found: 295.0598.

Molecular modeling

Homology modeling

The amino acid sequence Q8TET4 of *Homo sapiens* α -glucosidase (GANC) was retrieved from UNIPROT (Jain *et al.*, 2009). The template was chosen by running a psi-BLAST (Altschul *et al.*, 1997) of this sequence against Protein Data Bank (PDB). PDB 2QMJ, crystal structure of the human maltase-glucoamylase in complex with acarbose which showed sequence identity of 29% was chosen as template on basis of BLAST score, source organism and presence of inhibitor. The model was constructed and refined using MODELLER (Eswar *et al.*, 2006). Model refinement was primarily done using a rotamer library and loops were refined against a library of structures having high sequence identity with the template and its active site region. The quality of the constructed model at each step was cross-validated with Ramchandran plot (RAMPAGE) (Lovell *et al.*, 2003), energy profiles with ProSA (Wiederstein and Sippl, 2007; Sippl *et al.*, 1993) and the secondary structure was determined with STRIDE (Vriend, 1990).

Docking

The inhibitors and proteins were prepared using Schrodinger suite 2007 (Friesner *et al.*, 2004). Protein Preparation Wizard was used to prepare the proteins after adding the hydrogens with default settings. Ligands were submitted to confgen for conformational analysis followed by LigPrep (Schrodinger, 2005) module to generate a range of ionization states populated at a given pH range, i.e., ± 2 of 7.4. A grid of 10 Å box length was built with Asp 511 as grid center. The two modes of docking, simple precision (SP) and extra precision (XP) of Glide module was used. The default SP docking settings were used and the conformations obtained from SP were used as input for XP. Hydrophobic and hydrophilic maps were generated to get an idea of the solvent accessible regions.

QSAR

The molecules of the data set, were constructed by using standard geometries (standard bond lengths and angles) from the TRIPOS force field within the Sybyl 7.2 molecular modeling program (Rarey *et al.*, 1996). Charges were assigned using the Gasteiger–Marsili method. Energy minimization was performed using 20 simplex iterations followed by 1,000 steps of Powell minimization until the gradient norm 0.05 kcal/mol was achieved. Semiempirical AM1 method (Steward, 1993; Dewar *et al.*, 1985) was employed to obtain quantum mechanical descriptors and

given as input to CODESSA (Katritzky *et al.*, 1994) program where calculation and selection of descriptors for QSAR were carried out. A pool of 554 molecular descriptors of different types as constitutional, topological, geometric, electrostatic, and quantum-chemical was computed. After this calculation, the heuristic method was used to build different models before pinning down on the best predictive model for calculation of test set activities.

Biological activities

α -Glucosidase inhibitory assay

α -Glucosidase inhibitory activities were determined as per earlier reported methods (Rao *et al.*, 2009). Rat intestinal acetone powder in normal saline (100:1; w/v) was sonicated properly and the supernatant was used as a source of crude intestinal α -glucosidase after centrifugation. In brief, 10 μ l of test samples were reconstituted in 100 μ l of 100 mM-phosphate buffer (pH 6.8) in 96-well micro plate and incubated with 50 μ l of crude intestinal α -glucosidase for 5 min before 50 μ l substrate (5 mM, *p*-Nitrophenyl- α -D-Glucopyranoside prepared in same buffer) was added. Release of *p*-nitrophenol was measured at 405 nm spectrophotometrically (SpectraMax[®] plus384), Molecular Devices Corporation, Sunnyvale, CA, USA) 5 min after incubation with substrate. Individual blanks for test samples were prepared to correct background absorbance where substrate was replaced with 50 μ l of buffer. Control sample contained 10 μ l DMSO in place of test samples. Standard α -glucosidase inhibitor acarbose was taken as standard reference. All the samples we are studies in triplicate. Percentage of enzyme inhibition was calculated as $(1 - B/A) \times 100$ where $[A]$ represents absorbance of control without test samples, and $[B]$ represents absorbance in presence of test samples.

DPPH free radical scavenging activity

Assay for the scavenging of stable free radical 1,1-Diphenyl-2-picrylhydrazyl (DPPH) was done as reported earlier (Rao *et al.*, 2009). Briefly, in a 96-well micro plate, 25 μ l of test sample dissolved in DMSO, 125 μ l of 0.1 M tris-HCl buffer (pH 7.4) and 125 μ l of 0.5 mM DPPH solution dissolved in absolute ethyl alcohol were added. The reaction mixture was shaken well and incubated in dark for 30 min and read at 517 nm spectrophotometrically (SpectraMax[®] plus384, Molecular Devices Corporation, Sunnyvale, CA, USA). Trolox was taken as standard reference. All the samples we are studies in triplicate. Percentage of DPPH scavenging was calculated as $(1 - B/A) \times 100$ where $[A]$ represents absorbance of control without test samples, and $[B]$ represents absorbance in presence of test samples.

Animal experiment

Antihyperglycemic activity study was done according to the method reported earlier (Rao *et al.*, 2009). Wistar rats of either sex weighing between 195 and 215 g were obtained from National Institute of Nutrition (CPCSEA Reg. No. 154, Government of India), Hyderabad. The animals were housed in standard polyvinyl cages. The room temperature was maintained at $22 \pm 1^\circ\text{C}$ with an alternating 12 h light dark cycle. Food and water were provided ad libitum. Experiments were performed as per the Institutional Animal Ethical Committee norms. The rats were divided into various groups viz. control, test compound **8c** group (50 mg/kg body weight) and a group with standard drug Acarbose (10 mg/kg body weight). Five rats in each group were taken. All the animals were kept for overnight fasting. Next day forenoon blood was collected from retro orbital plexus in EDTA containing tubes, and plasma glucose levels for basal ('0' h) value were measured by glucose-oxidase test method using auto blood analyzer instrument (Bayer EXPRESS PLUS). Test sample and standard drug acarbose were suspended in normal saline and administered orally through gastric intubation. The control group of animals was treated sham with normal saline. Fifteen minutes after test sample treatment, animals were fed with soluble-starch dissolved in normal saline at a dose of 2 g/kg-body weight. Thereafter, blood was collected at intervals of 30, 60, 90, and 120th min post starch feeding. Plasma was separated out for glucose measurement as described above.

Acknowledgments We are thankful to the Dr. J. S. Yadav, Director, IICT for his constant encouragement. The author R. R. Rao is also grateful to CSIR, New Delhi, for the award of Research Fellowship. P.B. thanks DST for the Women Scientist Fellowship.

References

- Altschul FS, Madden TL, Schaffer AA, Zhang J, Zhang Z, Miller W, Lipman DJ (1997) Gapped BLAST and PSI-BLAST: a new generation of protein database search programs. *Nucl Acids Res* 25:3389–3402. doi:10.1093/nar/25.17.3389
- Anuradha V, Srinivas PV, Rao RR, Manjulatha K, Purohit GM, Rao JM (2006) Isolation and synthesis of analgesic and anti-inflammatory compounds from *Ochna squarrosa* L. *Bioorg Med Chem* 14:6820–6826. doi:10.1016/j.bmc.2006.06.048
- Aparna P, Tiwari AK, Srinivas PV, Ali AZ, Anuradha V, Rao JM (2009) Dolichandroside A, a new α -glucosidase inhibitor and DPPH free-radical Scavenger from *Dolichandrone falcata* seem. *Phytother Res* 23:591–596. doi:10.1002/ptr.2672
- Bharatham K, Bharatham N, Park KH, Lee KW (2008) Binding mode analyses pharmacophore model development for sulfonamide chalcone derivatives, a new class of α -glucosidase inhibitors. *J Mol Grap Model* 26:1202–1212. doi:10.1016/j.jmkgm.2007.11.002
- Boutati EI, Raptis SA (2004) Postprandial hyperglycaemia in type 2 diabetes: pathophysiological aspects, teleological notions and flags for clinical practice. *Diabetes Res Rev* 20:13–23. doi:10.1002/dmrr.528
- Ceriello A (2008) Cardiovascular effects of acute hyperglycaemia: pathophysiological underpinnings. *Diabetes Vasc Dis Res* 5:260–268. doi:10.3132/dvdr.2008.038
- Chinnaraju BC, Tiwari AK, Kumar JA, Ali AZ, Agawane SB, Saidachary G, Madhusudana K (2010) α -glucosidase inhibitory antihyperglycemic activity of substituted chromenone derivatives. *Bioorg Med Chem* 18:358–365. doi:10.1016/j.bmc.2009.10.047
- Chourasia M, Sastry GM, Sastry GN (2005) Proton binding sites and conformational analysis of $\text{H}^+ \text{K}^+ \text{-ATPase}$. *Biophysic Biochem Res Commun* 336:961–966. doi:10.1016/j.bbrc.2005.08.205
- Davidson J (2003) Should postprandial glucose be measured and treated to a particular target? Yes. *Diabetes Care* 26:1919–1921. doi:10.2337/diacare.26.6.1919
- Delorme S, Chiasson JL (2005) Acarbose in the prevention of cardiovascular disease in subjects with impaired glucose tolerance and type 2 diabetes mellitus. *Curr Opin Pharmacol* 5:184. doi:10.1016/j.coph.2004.11.005
- Dewar MJS, Zoebish EG, Healy EF, Stewart JJP (1985) Development and use of quantum mechanical molecular models. 76. AM1: a new general purpose quantum mechanical molecular model. *J Am Chem Soc* 107:3902–3909
- Eswar N, Marti-Renom MA, Webb B, Madhusudhan MS, Eramian D, Shen M, Pieper U, Sali A (2006) Comparative protein structure modeling using modeller. current protocols in bioinformatics. Wiley 15:5.6.1. doi:10.1002/0471250953.bi0506s15
- Friesner RA, Banks JL, Murphy RB, Halgren TA, Klicic JJ, Mainz DT (2004) Glide: a new approach for rapid, accurate docking and scoring. 1. Method and assessment of docking accuracy. *J Med Chem* 47:1739–1749. doi:10.1021/jm0306430
- Gerich JE (1996) Pathogenesis and treatment of Type 2 (noninsulin-dependent) diabetes mellitus (NIDDM). *Hormone Metab Res* 28:404–412. doi:10.1055/s-2007-979828
- Giugliano D, Ceriello A, Paolisso G (1996) Oxidative stress and diabetic vascular complications. *Diabetes Care* 19:257–267. doi:10.2337/diacare.19.3.257
- Goel A, Dixit M (2004) Amberlyst 15 catalyzed efficient synthesis of 5-acetyl-4-hydroxy-coumarone and 5-acetyl-6-hydroxy-coumarone: crucial precursors for several naturally occurring furanoflavones. *Synlett* 11:1990–1994. doi:10.1055/s-2004-831180
- Jain E, Bairoch A, Duvaud S, Phan I, Redaschi N, Suzek BE, Martin MJ, McGarvey P, Gasteiger E (2009) *BMC Bioinform* 10:136. doi:10.1186/1471-2105-10-136
- Katritzky AR, Lobanov VS, Karelson M (1994) CODESSA: reference manual; version 2. University of Florida, Gainesville
- Lovell SC, Davis IW, Arendall WB III, de Bakker PIW, Word JM, Prisant MG, Richardson JS, Richardson DC (2003) Structure validation by $C\alpha$ geometry: φ ψ and $C\beta$ deviation. *Proteins Struct Funct Genet* 50:437–450. doi:10.1002/prot.10286
- Matsui T, Ogunwande I, Abesundara KJM, Matsumoto K (2006) Anti-hyperglycemic potential of natural products. *Mini Rev Med Chem* 6:109–120
- McCarty MF (2000) Toward practical prevention of type 2 diabetes. *Med Hypotheses* 54:786. doi:10.1054/mehy.1999.0952
- Milisevic Z, Raz I, Beattie SD, Campaigne BN, Sarwat S, Gromnaik E, Kowalska I, Galic E, Tan M, Hanefeld M (2008) Natural history of cardiovascular disease in patients with diabetes: Role of hyperglycemia. *Diabetes Care* 2:155–160. doi:10.2337/dc08-s240
- Mishra A, Khurana L, Isharwa S, Bhardwaj S (2009) South Asian diets and insulin resistance. *Br J Nutr* 101:465–473. doi:10.1017/S0007114508073649
- Mohan V, Radhika G, Sathya RM, Tamil SR, Ganesan A, Sudha V (2009) Dietary carbohydrates, glycaemic load, food groups and

- newly detected type 2 diabetes among urban Asian Indian population in Chennai, India. *Br J Nutr* 102:1498–1506. doi:10.1017/S0007114509990468
- Murthy JN, Nagaraju M, Sastry GM, Rao AR, Sastry GN (2005) Active site acidic residues and structural analysis of modelled human aromatase: A potential drug target for breast cancer. *J Comp Mol Design* 19:857–870. doi:10.1007/s10822-005-9024-0
- Rao RR, Tiwari AK, Reddy PP, Babu KS, Ali AZ, Madhusudana K, Rao JM (2009) New furanoflavonoids, intestinal alpha-glucosidase inhibitory and free-radical (DPPH) scavenging activity from antihyperglycemic root extract of *Derris indica* (Lam.). *Bioorg Med Chem* 17:5170–5175. doi:10.1016/j.bmc.2009.05.051
- Rarey M, Kramer B, Lengauer T, Klebe G (1996) A fast flexible docking method using an incremental construction algorithm. *J Mol Biol* 261:470–489
- Ravindra GK, Achaiah G, Sastry GN (2008) Molecular modeling studies of phenoxyimidazole as p38 kinase inhibitors using QSAR and docking. *Eur J Med Chem* 43:830–838. doi:10.1016/j.ejmech.2007.06.009
- Reddy ChS, Vijayasarathy K, Srinivas E, Sastry GM, Sastry GN (2006) Homology modeling of membrane proteins: a critical assessment. *Comp Bio Chem* 30:120–126
- Rodbard HW, Jellinger PS, Daivison JA, Einhorn D, Garber AJ, Grunberger G, Handelsman Y, Horton ES, Lebovitz H, Levy P, Moghissi ES, Schwartz SS (2009) Statement by an American Association of Clinical endocrinologists/american college of endocrinology consensus panel on type 2 diabetes mellitus: an algorithm for glycemic control. *Endocrinol Pract* 15:540–559
- Saxena DB, Tomar SS, Singh RP, Mukerjee SK (1987) A new chalcone from *Millettia ovalifolia*. *Indian J Chem* 26B(7):704
- Schrodinger (2005) LigPrep, version 2.1. Schrodinger, New York
- Selvam JJP, Rajesh K, Suresh V, Babu DC, Venkateswarlu Y (2009) A new synthesis of the phytotoxic 10-membered lactone herbarumin I. *Tetrahedron Asymmetr* 20:1115. doi:10.1016/j.tetasy.2009.03.034
- Sritularak B, Likhitwitayawuid K (2006) Flavonoids from the pods of *Millettia erythrocalyx*. *Phytochemistry* 67:812–817. doi:10.1016/j.phytochem.2006.01.013
- Srivani P, Sastry GN (2009) Potential choline kinase inhibitors: a molecular modeling study of bis-quinolinium compounds. *J Mol Graph Mod* 27:676–688. doi:10.1016/j.jmgm.2008.10.010
- Steward JJP (1993) MOPAC 93 annual revision number 2. Fujitsu, Tokyo
- Talapatra SK, Mallik AK, Talapatra B (1982) Isopongaglabol and 6-methoxyisopongaglabol, two new hydroxy furanoflavones from *Pongamia glabra*. *Phytochemistry* 21:761–766. doi:10.1016/0031-9422(82)83183-X
- Vriend G (1990) What if: a molecular modeling and drug design program. *J Mol Graph* 8:52–56. doi:10.1016/0263-7855(90)80070-V
- Wiederstein M, Sippl MJ (2007) ProSA-web: interactive web service for the recognition of errors in three-dimensional structures of proteins. *Nucl Acid Res* 35:W407–W410. doi:10.1093/nar/gkm290
- Yamagishi S, Nakamura K, Takeuchi M (2005) Inhibition of postprandial hyperglycemia by Acarbose is a promising therapeutic strategy for the treatment of patients with the metabolic syndrome. *Med Hypotheses* 65:152–154. doi:10.1016/j.mehy.2004.12.008
- Zhitao Li, Ngojeh G, De Witt P, Zheng Z, Chen M, Lainhart B, Vincent Li, Felipo P (2008) Synthesis of a library of glycosylated flavonols. *Tetrahedron Lett* 49:7243–7245. doi:10.1016/j.tetlet.2008.10.032